Transcriptome Profiling and Gene Network Analysis Revealed Regulatory Mechanisms of Bract Development in Bougainvillea glabra

xiangdong liu
Hunan Agricultural University
Yaonan Peng
Hunan Agricultural University
Qinghui Zeng
Hunan Agricultural University
Yuwan Ma
Hunan Agricultural University
Jin Liu
Hunan Agricultural University
Yaqi Huang
Hunan Agricultural University
Xiaoying Yu
Hunan Agricultural University
Jun Luo
Hunan Botanical Garden
Yanlin Li
liyanlin@hunau.edu.cn
Hunan Agricultural University
Meng Li
Central South University of Forestry and Technology
Fuxiang Cao
Hunan Agricultural University

Research Article

Keywords: Bract development, Bougainvillea glabra, MADS-box, Squamosa promoter binding protein (SBP), Plant hormone signal transduction, Chlorophyll Metabolic Pathways

Posted Date: April 26th, 2024

DOI: https://doi.org/10.21203/rs.3.rs-4275941/v1

Additional Declarations: No competing interests reported.

Abstract

Background: Bracts are important in ornamental plants and their developmental regulation is complex, but relatively little research has been done on them. In this study, physiological, biochemical and morphological changes in *Bougainvillea glabra*leaves, leaf buds and bracts during seven developmental periods were systematically investigated in *B. glabra* bracts. Meanwhile, transcriptome data of *B. glabra* bracts were obtained using PacBio and Illumina sequencing technologies, and key genes regulating their development were screened.

Results: Scanning electron microscopy revealed that the bracts develop with a process of regression of hairs, changing colour from green to white; Transcriptome sequencing yielded 79,130,973 bp of transcript sequences, totalling 45,788 transcripts; Differential gene analysis revealed 50 expression patterns across seven developmental periods, with significant variability in transcription factors such as *BgAP1*, *BgFULL*, *BgCMB1, BgSPL16*, *BgEIL1,* and *BgBH305* KEGG and GO analyses of growth and development concerning chlorophyll metabolism and hormone-conducting metabolic pathways; Key genes for chlorophyll metabolism include *PORA*, *SGR*, *PPH*, *PAO* and *RCCR*; The growth hormone and abscisic acid signalling pathways involve 44 and 23 homologous genes, and co-expression network analyses revealed that the screened genes *BgAPRR5* and *BgEXLA1* are involved in the regulation of bract development.

Conclusions: These findings promote the understanding of the molecular mechanism of plant bract development, as well as provide important guidance for the molecular regulation and genetic improvement of the growth and development of ornamental plants, mainly ornamental bracts.

Introduction

Bract is the metamorphosed leaf that appears accompanying inflorescence. In general, any leaf associated with inflorescence can be defined as a bract[1,2]. Strictly speaking, bract does not belong to the inflorescence structure, while it can be considered as an extension of floral organs. The bract primordia originated from the stem meristem usually generated at the very early stage of reproductive development [3]. However, a “bract suppression system” has been observed in many, but not all, angiosperm species. This system will cease the development of the bract and eventually subsume the bract primordia into the floral meristem. Therefore, bract is absent in many model plants, such as *Arabidopsis*, maize (*Zea mays*) and rice (*Oryza sativa*). The bract development system has been suppressed rather than removed in these higher plants. Moreover, a study in rice indicated that bract suppression is not only necessary for floral development but also critical for the transition from vegetative to reproductive branching[4,5]. Although bract suppression is a conserved mechanism in most angiosperm lineages, some plants are retaining the trait of natural bract development, such as species belonging to the *Cornaceae*, *Nyssaceae, Nyctaginaceae* and *Araceae families*.

In many ornamental plants, the bract is an important organ undertaking reproductive events, as well as an ornamental character[6]. The bract with ornamental value is called a petaloid bract, which results from

the ectopic expression of genes determining the petal identity in the leaf. This process is supposed to involve the developmental signals transduction and the activation or suppression of related genes. Ectopic petalization (petal-like characteristics in non-petal organs) contributed to the diversity of flower morphology in the process of angiosperm evolution. The MADS-box gene family belonging to the B-class of the ABC model has been verified to play a key role in ectopic petalization. A MADS-box gene, *AGL6*, was identified to regulate floral organ development and flowering time in *Arabidopsis* [7]. Overexpression of the *AGL6* gene in *Arabidopsis* promoted the growth of petal-like bracts. Similarly, ectopic expression of the MADS-box genes was observed in *Cornus officinalis*. Significant upregulation of the *CorPI-B*, *CorPI-A* and *CorAP3* genes was detected in the *C. officinalis* bracts along with the developmental stages[8,9]. In *Aristolochia* (Aristolochiaceae, basal angiosperm), expression of an *AP3-like* gene was detected only during the late stages of petaloid perianth development and expression of B-class paralogs was detected in late development of Aquilegia petaloid sepal[10]. The *JAGGED* gene is the only gene that has been reported to positively regulate bract development in *Arabidopsis*. Overexpression of the *JAGGED* gene promoted bract development in *Arabidopsis*, and bract development was inhibited in the *APETALA1*(*AP1*) *jagged* double mutant [11]. A recent study has identified a bract-specific gene, *DiASR1* (abscisic acid, stress and ripening protein), from the dove tree (*Davidia involucrata*). Overexpression of the *DiASR1* gene induced bract-like leaves in *Arabidopsis*[2]. Although there is a large body of literature on bract development, most of it focuses on bract inhibitory systems and is carried out in model plants, whereas the mechanism of natural bract development remains largely unknown. More genes regulating bract development are expected to be explored in those naturally bracted species.

Ornamental plant bracts are currently more studied mainly in pigments, For example, *Bougainvillea* is a woody plant of the *Nyctaginaceae*[12], rich in colour, such as chalcone--flavonone isomerase 1(*CHI1*), 4,5-DOPA dioxygenase extradiol (*DOD*) and flavanone 3-hydroxylase(*F3H*), have all been shown to be involved in bract colour change[13,14]. But there is very little research on how bracts develop. However, the molecular mechanism underlying the key events of bract development, including organogenesis, chloroplast degeneration, petal identity determination, rapid growth and abscission needs integrative investigation. *B. glabra* 'Mrs. Eva White' bracts have significant ornamental value. Its bracts are large and thin, making it ideal for studying bract development. To unravel the developmental mechanisms of bracts in ornamental plants. We conducted a comprehensive analysis of *B. glabra* 'Mrs. Eva White' at the morphological level and transcriptome to identify key genes involved in these processes.

Results

Morphological and photosynthetic pigment changes during bract development in B.glabra

The development of *B. glabra* buds was found to go through five main periods as observed by resin sections. At the initial stage, it contains only bracts and growth points (Fig. S1A-a). The primordium forms the outermost whorl of the inflorescence, around which the primordium of the bracts appears in rapid succession and consists of outer and inner cells, the former being larger and looser, the latter

smaller and more compact, followed by a gradual growth of the flower primordium (Fig. 1B-a). The floret primordium rapidly differentiates ((Fig. S1A-b) and the perianth whorl begins to appear around the primordium (Fig. 1A, S1A-b). The floral organs develop further, the buds expand, the sepals and petals gradually elongate, the growth cone broadens, the outer petals differentiate into small projections, and the stamen primordia begin to form (Fig. 1B-c). During the LB period（Late Bud）, the stage of bract protocorm differentiation, the androecium has not yet completed its differentiation and is still in the protocorm stage (Fig. S1B-a). Subsequently, androgynous differentiation is completed, and this process is known as the stage of floral primordium differentiation (Fig. S1B-b).

Scanning electron microscopy showed that bract villi gradually degenerated during development(Fig. 1C). During the BR1 period, the villi were dense and gradually decreased as the bracts developed (Fig. S1C). The development of *B. glabra* bracts shows a slow-fast-slow pattern. The bracts were initially green and then showed a change in chlorophyll degradation. From the onset of bract primordium, growth is slow for the first 5 days, accelerates on day 6, and enters a period of rapid growth on day 17, when the bracts gradually change from green to white (Fig. 1D). Chlorophyll content tended to decrease during development, especially significantly from bract period 2, indicating that bract development was accompanied by a process of chlorophyll regreening. However, the chlorophyll content of bracts increased slightly during senescence. Overall, the chlorophyll and carotene content of *B. glabra* bracts was significantly lower than that of the leaf blade (Fig. 1E).

Transcriptome sequencing and sequence analysis of leaf buds, leaves and bracts at different developmental periods

In this study, the samples were subjected to transcriptome sequencing using the Circular Consensus Sequence Technique, which yielded a total length of 1041,643,869bp of the circular consensus sequence. The homologues and polyA tails were removed by Isoseq processing and 463,177 FLNC reads were obtained. Subsequently, the FLNC sequences were clustered and de-redundant using the ICE tool of SMRTlink software, resulting in a non-redundant transcript sequence of 79,134,466bp. Thereafter, to improve sequence accuracy, the transcript sequence was further corrected using LoRDEC error correction software, resulting in a corrected transcript sequence of 79,130,973bp.

After obtaining the transcript sequences, they were clustered and de-redundant using cd-hit software to create the final full-length transcript sequences, which were used as the reference transcript sequences for second-generation data comparison. The comparison results showed that a total of 45,788 transcripts were detected in the samples, with a total base of 706,647,796 bp and an average length of 1,544 bp. These findings provide an important database for subsequent transcriptome analyses.

Transcriptome differential gene analysis

Principal Component Analysis (PCA) of the gene expression levels (FPKM) of all the samples revealed that the samples from the LB, FB and BR1 periods clustered together, whereas the BR2 period began to show a trend of dispersion. Over time, samples from the BR3, BR4 and BR5 periods showed more similar

gene expression patterns. However, samples from the LE and BR6 periods showed a clear trend of separation from the other periods (Fig. 2A).

Analyses for differentially expressed genes between LB/FB, FB/BR2, BR2/BR5 and BR5/LE revealed 245 differentially expressed genes between LB/FB and 2,039 differentially expressed genes between FB/BR2. 3,769 differentially expressed genes were found between BR2/BR5 (Fig. 2B). Subsequently, these 37,842 differentially expressed genes were analysed by clustering expression trends over time using STEM software. The results showed that these differentially expressed genes exhibited 50 different expression patterns within 7 periods. Among them, 20709 differentially expressed genes showed 8 significantly clustered expression patterns ($P < 0.05$). The more critical of these patterns include expression pattern I, which is down-regulated, and expression pattern II, which is down-regulated and then up-regulated. In addition, differential genes in expression pattern 22 were up-regulated from BR1 to BR2, then down-regulated from BR2 to BR3, and then up-regulated from BR3 to BR4 and BR5 to BR6, while expression pattern 8 showed a trend of down-regulation followed by up-regulation (Fig. 2C).

Analysis by GO enrichment showed that these differentially expressed genes were involved in important pathways such as reproduction, reproductive processes and growth (Fig. 2D). The SBP and MADS-box families were mainly involved. Among them, members of the MADS-box family include *BgAP1*, *BgFULL*, and *BgCMB1*, etc., while members of the SBP family include *SPL16*, *SPL8*, and *SPL14*, etc. (Fig. 2E, F, G). These results further revealed the important role of gene expression regulation in plant bract development. The metabolic pathways related to bract development were found to be mainly porphyrin and chlorophyll metabolism, Plant hormone signal transduction and other metabolic pathways by KEGG enrichment analysis (Fig. 2H, Fig. S2).

Chlorophyll Metabolic Pathways During Bract development

B. glabra 'Mrs. Eva White' bracts evolve in colour from green to white during their development, a transition that is regulated by chlorophyll metabolism. Chlorophyll metabolism consists of three main processes: synthesis, recycling and degradation. As can be seen in Figure 3, in the synthetic pathway, hydroxymethyl chlorophyll was gradually reduced to Chlorophyllide by the catalysis of *NADPH-POR.PORA* was highly expressed in the early stage of bract development and gradually decreased to very low levels as development progressed, suggesting that the ternary complex formed by hydroxymethyl chlorophyll a, *NADPH*, and *POR* is the key to the green colour of bracts in the early stage of bract development. The genes found to interact with *PORA* by differential protein network analysis were *PPOC*, *PAO*, and *BgCHLH* (Fig. S3). The expression of *SGR*, *PPH*, *PAO* and *RCCR* genes was low at the early stage of bract development, and then gradually increased, especially at the BR3 and BR4 stages. Therefore, it can be hypothesized that this period is the critical period for bracts to change from green to white.

Metabolism of auxin and Abscisic Acid during bract development

Endogenous plant hormones play an important role in leaf development and have a regulatory role in the development of *B. glabra* bracts. Further in-depth analysis of the plant hormone signalling pathways led

to the detection of a large number of differential genes involved in hormone signalling response and transduction at key sites of bract formation. These genes are involved in a variety of hormones such as auxin, Abscisic Acid, cytokinin, gibberellins, ethylene, and jasmonic acid.

Indole-3-acetic acid (IAA) synthesis can be divided into the tryptophan-dependent pathway and the tryptophan-independent pathway. In the growth hormone signal transduction pathway, we further identified 44 homologous genes that encode 12 enzymes in the growth hormone synthesis pathway. The tryptophan-independent pathway includes two encoding *ASB1* and *TRPX*, five encoding *PAT1*, two encoding *PAI1*, and six encoding *TRPC* genes. The *TRPX*, *ASB1*, *PAT1*, *PAI1*, *PRPC*, and *TRA2* genes in this pathway are all highly expressed in the early stages of bract development and decrease in the later stages. The tryptophan-dependent pathway includes 15 coding *TRPB*, 4 coding *TIR1*, 3 coding *AMI1*, and 3 coding *ALDO2*, *TAR1*, *YUC*, and *TRPA2* all with only 1 code. The expression of the *YUC* and *AMI1* genes of this pathway was higher in the early stage, The *YUC* gene started to decline gradually in the BR2 period, while the *AMI1* gene started to decline gradually in the BR3 period, and the expression of the *ALDO2* gene increased with bract development. These results suggest that they may play an important regulatory role in bract development (Fig. 4).

In the abscisic acid signalling pathway, we further identified 23 homologous genes encoding four enzymes based on the growth hormone synthesis pathway. These include 2 encoding *ECED2*, 3 encoding *ECED1*, 5 encoding *ALDO3* genes, and 12 encoding *ABA2*. *NCED2* was up-regulated during BR5 *NCED1* and *ALDO3* genes were up-regulated during BR6.The *ABA2* base was up-regulated during early development. Therefore, it is inferred that these genes play an important regulatory role in bract senescence (Fig. 5)

Weighted correlation network analysis （WGCNA analysis）

A systems biology approach using weighted gene WGCNAs was used to construct WGCNAs, which included 12,370 genes (FPKM ≥ 10) and 1,506 transcription factors, as a way to reveal the function of the network. In this network, the blue and brown modules showed a significant negative correlation with bract area and chlorophyll content, while the variability was particularly significant for the red and brown modules (Fig. 6A, Fig. S4).

Several key HUB genes were identified, including *Bg_3140*, *Bg_11315*, and *Bg_23959* in MEblue (Fig. 6B, Fig. S5), and transcription factor HUB genes *Bg_26128* and *Bg_10088* in MEbrown (Fig. 6C,Fig. S6), with structural genes with HUBs mainly *Bg_23913* and *Bg_37656* (Fig. 6D). Notably, the HUB genes *BgPORA* and *BgEXLA1* showed significant expression differences during BR1. Among them, the HUB gene *EXLA1* encodes an expansion protein that plays an important role in plant cell wall relaxation and regulates the expansion of *B. glabra* bract cells. The HUB gene *POR*A, on the other hand, is a key gene in the process of chlorophyll metabolism and is involved in the biosynthesis of light-sensitive pigments by regulating the expression of *POR*A, which in turn affects chlorophyll biosynthesis, which is consistent with chlorophyll degradation during bract development in Trigonella foetidum(Fig. 6D).

In addition, we also found that the brown module HUB genes mainly included *BgBZP44, BgAPRR5* and *BgIAA7*, which were related to the regulation of phy B photoreceptors and the regulation of plant growth hormones. During the development of *B. glabra* bracts, *APRR5* showed a gradually increasing trend, especially with high expression levels during the BR6 period (Fig. 6E). *BgTLP8*, *BgAPRR2*, *BgBZP44*, *BgEXLA1*, and *BgPORA* are highly expressed in the blue module during the early stages of bract development, which plays an important role in the regulation of *B. glabra* bract development and senescence and other processes.

qRT-PCR of bract development-related candidate genes

Based on the above analysis, we performed qRT-PCR on one structural gene and eight transcription factors of the screened chlorophyll metabolic pathway. qRT-PCR results were also compared with RNA-seq (FPKM) results to verify the consistency of the gene expression pattern with the sequencing results. The results showed that the results were similar to the expression trends obtained by RNA-Seq(Fig. 7).

Discussion

Involvement of MADS-box in *B. glabra* bract development

There are more studies on flower development, but relatively few studies on bract development in ornamental plants, and the molecular mechanism of their bract development is still unclear. MADS-box proteins are a large family of transcription factors that play key roles in eukaryotic development, regulating the intensity of target gene expression in a given time and space by binding to cis-acting elements that interact with the target gene[15].In this study, we found that the differentially expressed genes *BgAP1*, *BgCMB1*, *BgDEFA*, and *BgFULL* were all in the MADS-box family during the development of *B. glabra* bracts and that the expression of *BgAP1* was largely inversely related to that of *BgFULL*. It has been suggested that *FRUITFULL*(*FULL)* is negatively regulated by *AP1* during the early stages of *Arabidopsis thaliana* development. *FULL* is hardly expressed in early trophic organs until after the onset of inflorescence development [16]. *AP1* represses *FULL* expression during sepal and petal development.AP3, on the other hand, inhibits the expression of *FULL* in stamen development [17]. Although it is unclear whether there is negative regulation of *FULL* by *AP1* during bract development, it is hypothesised that there may be mutual regulation of *BgAP1* and *BgFULL* based on their expression patterns at different developmental periods. Specifically, *BgAP1* was expressed mainly in the later stages of bract development, whereas *BgFULL* was expressed in the early stages of bract development. It is more consistent with the results of previous studies. While most of the MADS-box genes are expressed only in flowers, *FULL* is expressed at different specific stages of bract development. Investigations in a variety of plant species suggest that the requirement for B-class gene function during heterotopic petaloidy varies dramatically, and may function early, late, or not at all during the development of petaloid organs[18,19]. In *Aristolochia* (*Aristolochiaceae*, basal angiosperm), expression of an *AP3-like* gene was detected only during the late stages of petaloid perianth development and expression of B-class paralogs

was detected in late development of *Aquilegia* petaloid sepals, suggesting that B-class homologs may only be required relatively late in the development of petaloid organs in these species[20].

CMB1 is a gene of the MADS-box family, be involved in the regulation of pistil and sepal development in some plants. It has been suggested that *PpCMB1* regulates pistil and sepal development in *Prunus persica*[21]*.CMB1* is involved in fruit ripening and sepal development[22]; In *Solanum lycopersicum,* it was studied that *SlCMB1* is a SEP-like MADS-box gene involved in inflorescence and sepal development by interacting with other genes [23]. In this study, the expression of *BgCMB1* was found to trend upward with bract development and was positively correlated with *BgAP1* expression. *BgAP1, BgFULL, BgCMB1, and BgDEFA* were barely expressed in leaves but were highly expressed during bract development. These results suggest a potential role for *BgCMB1* in bract development and may be related to the fact that *BgCMB1* interacts with *BgAP1* and *BgFULL* to regulate bract development.

SBP family involved in *B. glabra* bract development

SBP is a plant-specific class of transcription factors that are closely related to plant inflorescence development and yield[24].SBP proteins have a zinc finger structure that recognises and binds to the promoter of the MADS-box gene SQUAMOSA (SQUA), which is involved in plant growth and development as well as a variety of physiological and biochemical processes. In addition, SBP a class of transcription factors can regulate flower and fruit development [25]. In *A. thaliana*, SBP homologues *SPL3*, *SPL4* and *SPL5* regulate *A. thaliana* flower development, whereas the *SPL8* and *SPL14* genes regulate pollen development [26], which in turn affects yield.

The MADS-box transcription factor *FULL*, together with the SBP transcription factor, plays a role in reproductive transformation and meristem identity transformation[27]. *AtSPL3* in *A. thaliana* was identified as a direct upstream activator of *FULL* and the activation of *FULL* by *SPL3* was very strong [28]. In *A. thaliana* Yamasaki also demonstrated that *AtAP1* is downstream of the *AtSPL3* gene [29]. Further studies showed that after silencing and overexpression of the *PpSPL16* gene in *P. persica*, the expression of the *PpFULL* and *PpAP2a* genes were down-regulated and up-regulated, respectively, which further regulated fruit ripening in *P. persica* through the regulation of the *PpFULL* and *PpAP2a* genes [30]. Whether *SPL16* interacts with *FULL* during bract development is unknown, but the analyses in this study revealed that both *BgSPL16* and *BgAP1* as well as *BgSPL16* have a crucial role in *B. glabra* bract development. In this study, the *BgSPL* genes showed different temporal and spatial expression patterns. The high expression levels of *BgSPL8*, *BgSPL13* and *BgSPL16* at the stage of floral differentiation further confirmed the role of SPLs in regulating the asexual to reproductive transition through different regulatory roles during flower bud differentiation.*SPL3* does not play a major role in asexual changes or at anthesis, but it promotes a shift in floral phloem identity by activating floral phloem-specific genes[31].In addition, *SPL7* and *SPL8* induced phase transition and flowering in Gramineae by directly upregulating *SEPALLATA3* (*SEP3*) and *MADS32*[32]**.** It was also found that *SPL8* was involved in GA signalling and positively regulated trichome formation on sepals and stamen filament elongation [33]. In this study, we

found that *BgSPL8* was expressed in bracts but not in leaves during bract development, and *BgSPL16* was highly expressed during the FB period, with lower expression at other periods. Therefore, the present study hypothesized that *BgSPL8* and *SPL16* are associated with bract development, which provides important clues for further studies on plant growth and development.

Chlorophyll metabolism during bract development in *B. glabra*

In this study, it was found that *B. glabra* 'Snow White' bract pigmentation consisted of chlorophyll, carotenoids, and Flavonoids, and that at the beginning of the developmental stage *B. glabra* bracts had a high content of chlorophyll, but as the bracts developed, the colour gradually changed to white. Currently, phytochrome-mediated light signalling has been reported to induce *PORA* gene expression in *Monocotyledons* such as *Hordeum vulgare* and similarly in dicotyledons such as *A. thaliana* [34,35]. Meanwhile, it has been suggested that *PORA* is abundant in yellowing plants, is active mainly during seedling de-yellowing, and acts synergistically with the light-trapping complex[36]. Identified a mutant type in *A. thaliana* with yellow leaves that do not turn green when grown in white light, confirming that the presence of *PORA* confers a certain degree of photoprotection to the plant. The *PORA* of Pchlide is the only step of light-requiring enzyme mediating the biosynthesis of chlorophyll in higher plants[37], and its expression is regulated by photosensitive pigments, thus affecting chlorophyll biosynthesis. This study further reveals that *BgPORA* may be a key gene for chlorophyll formation during bract development.

In addition, STAY-GREEN Proteins(*SGR*), play key regulatory roles in chlorophyll degradation and function independently of *PAO* enzymes. Meanwhile, chlorophyll degrading enzymes including *PPH*, *PAO* and *RCCR*, the genes for which have been identified in model crops such as *Oryza sativa*, *A. thaliana*, etc., and the alteration of their transcriptional expression levels affect the process of chlorophyll degradation, and consequently the yellowing or senescence phenotypes of the leaves. It has been suggested that knockdown or inhibition of *SGR* expression delays chlorophyll degradation, leading to a stagnant green phenotype in plants during natural development or dark-induced senescence [38]. In this study, *B. glabra* bracts were found to be up-regulated during development with *SGR* in the later stages of *B.glabra* bract development, which may be a key gene regulating bract greening to whitening.

Effects of auxin and Abscisic Acid during bract development

Auxin is a Phytohormone that plays an important role in plant growth and development. It has an unsaturated aromatic ring and an acetic acid side chain, in which indole-3-acetaldoxime can be converted to indole-3-acetaldehyde, and can be catalytically generated into IAA by *ALDO2* enzyme. This pathway is currently relatively understudied, especially concerning bract development. The indole-3-pyruvic acid pathway(IPA) is the main pathway for IAA biosynthesis in plants and is widely present in most plant bodies[39]. It has been shown that *YUCCA* (*YUC*) is involved in the IPA pathway in synergy with tryptophan aminotransferase of Arabidopsis (TAA), in which TAA is involved in catalysing the conversion of tryptophan to IPA, and subsequently, *YUC* is involved in catalysing the production of IAA from IPA[40,41].

The *YUC* and TAA families mainly regulate embryonic development after the spherical embryo stage[42].In this study, we found that the *BgYUC* gene is highly expressed mainly in the prophase of the growth hormone synthesis pathway and plays a regulatory role in the prophase of bract development. In this study, we hypothesised that *YUC* expression in this pathway is high in the early stages of bract development and low in the later stages, and its molecular mechanism with bract development remains to be investigated.

Abscisic Acid metabolic pathway mainly includes the Terpenoid pathway and the Carotenoid pathway [43]. The terpenoid pathway, also known as the C15 direct pathway, consists of the direct formation of 15-carbon ABA from FARNESYLPYROPHOSPHATE (FPP) via cyclisation and oxidation whereas the carotenoid pathway, also known as the C40 indirect pathway, is the main pathway for major ABA synthesis in higher plants. In this pathway, the conversion of zeaxanthin to violaxanthin is catalysed by zeaxanthin epoxidase(ZEP)which is followed by 9-cis-epoxy carotenoid dioxygenase(NCED)which catalyzes the production of xanthoxin from 9-cis-neoxanthin. The short-chain alcohol dehydrogenase *ABA2* converts to ABA-aldehyde, which is ultimately converted to ABA by *ALDO3*[44].In this study, we found that Bg*ALDO3* was highly expressed during the BR6 period at the end of bract development, suggesting that bract senescence is associated with Bg*ALDO3*.It has been suggested that the ABA signalling pathway is associated with PSEUDO-RESPONSE REGULATOR5 (*APRR5*) and *APRR7* and that *ABI5*, a key regulator in the ABA signalling pathway, specifically interacts with *APRR5* and *APRR7*[45].In this study, *BgAPRR5* was found to be highly expressed during the BR6 period, and it was hypothesised that this gene is associated with the Abscisic Acid metabolic pathway, which provides important clues for understanding the molecular mechanisms of plant Auxin and Abscisic Acid in bract development.

Conclusion

In conclusion, our investigation into the development of *Bougainvillea glabra* bracts has identified critical physiological and genetic mechanisms. We observed key changes in bract morphology, including increased area and chlorophyll content, accompanied by a reduction in hairiness (glabrescence). These morphological changes correlate strongly with the dynamics of hormone transduction pathways and chlorophyll metabolism. Importantly, genes within the MADS-box and SBP families, such as *BgAP1*, *BgFULL*, *BgSPL16*, *BgCMB1*, and *BgDEFA*, play pivotal roles in these developmental processes. Our study also highlights the significance of *BgPORA* and *BgSGR* genes in the biosynthesis and breakdown of chlorophyll during bract development. The expression patterns of *BgPRPC* and *BgTRA2* suggest their involvement in early developmental stages through both tryptophan-dependent and independent growth hormone pathways. Furthermore, the up-regulation of *BgALDO3* during the BR6 period underscores its potential importance in later developmental stages, particularly in the abscisic acid pathway. These findings not only enhance our understanding of bract development in *B. glabra* but also suggest avenues for future research to explore the regulatory mechanisms of floral architecture in ornamental plants.

Materials and methods

Plant material, sample collection

B.glabra 'Mrs. Eva White' planted in the flower base of Hunan Agricultural University was selected as the plant material for this study in August 2021, and the different developmental stages of the bracts were divided into eight stages of bract sample collection (Fig. 1A). Three plants were set up as 1 biological replicate, and 3 biological replicates were obtained at each developmental stage. Twenty representative samples were collected from each biological replicate and mixed. These samples were immediately placed in liquid nitrogen and stored in a refrigerator at -80°C for RNA extraction and then sent to Fraser Bioinformatics for sequencing using a PacBio sequencer.

Microscopic observation, paraffin sections, scanning electron microscopy methods

Dissection of delphiniums at the time of flower bud point to observe their internal structure. Buds from LB and FB periods were selected for paraffin sectioning, Samples from the LB and FB periods were taken and soaked in FAA fixative, and the follow-up experiments were entrusted to Wuhan Safeway Biotechnology Co. To understand the flower bud development for the resin section, collect buds in different periods, immediately soak in FAA fixative (70% ethanol: glacial acetic acid: formaldehyde: 90:5:5) fixed, dehydration after completing using Technovit 7100 resin embedding kit for embedding, embedding after using Leica EM UC6 section, using 0.1% toluidine blue dye solution for staining with the microscope. To observe the phenotypic changes of bract development, samples were taken from BR1, BR3, BR5, LE period for electron microscopy scanning, and the subsequent experiments were entrusted to Wuhan Sevier Biotechnology Co.

Bract area, chlorophyll measurement

The rate of bract development was observed daily, and the area of delphinium bracts was measured using a leaf area meter. The chlorophyll and carotenoid contents of leaf buds, leaf blades and bracts at different periods of development were determined by Ultraviolet-visible Spectrophotometer, respectively. Several samples were harvested, washed and cut into strips of about 2 mm, weighed 0.2 g, and extracted in 95% ethanol for 24 hours, and three replicates were set up for each species in each treatment. After 24 hours, the absorbance at 470 nm, 665 nm and 649 nm was measured by Ultraviolet-visible Spectrophotometer, and the content of chlorophyll a, chlorophyll b and carotenoids were calculated.

Iso-Seq analysis method

Total RNA was extracted from the tissue samples, the concentration and purity of the extracted RNA were tested by Nanodrop 2000, genomic contamination, purity and RNA integrity of the samples were detected by agarose gel electrophoresis, and the RIN values were determined by Agilent 2100. High-quality RNA is the basis for successful sequencing. To ensure the accuracy of the sequencing data, the samples were tested and the results met the requirements before library construction. After library testing, full-length transcriptome sequencing was performed using a PacBio sequencer according to the target downstream

data volume. Raw sequencing data were preprocessed using SMRTlink software and full-length transcript sequences were obtained using the Iso-Seq analysis process.

Identification of Coexpression Modules and Visualization of Hub Genes

The weighted gene correlation network analysis (WGCNA) package in R was used to construct the gene co-expression network analysis for *Bougainvillea* based on the gene-level FPKM data from differentially expressed genes during the 8 bract developmental stages. Module detection was performed using the TOM-based similarity measure and the dynamic tree-cutting algorithm to cut the hierarchal clustering tree and define modules as branches from the tree cutting.

The minimum number of genes per module was set as 30 genes by default, and the threshold of module merging correlation for eigengene similarity was 0.9 (Fig. S7). module-tissue association analysis, the eigengene value was calculated for each module and used to test the association with each tissue type. The total connectivity and intramodular connectivity, kME, and kME-p-value were calculated and represent the Pearson correlation between the expression level of that gene and the ME. Additionally, genes with the highest degree of intramodular connectivity within a module are referred to as hub genes. The networks were visualized using Cytoscape_v.3.8.0.

Quantitative real-time PCR

The *BgActin* gene was used as the internal control. Primers used in the study are listed in Supplemental Table S1. Real-time fluorescence quantitative qPCR was performed using (the ChamQ Universal SYBR qPCR Master Mix) kit. The relative gene expression levels were normalized using the $2^{-\Delta\Delta Ct}$ method.

Data analysis

The experimental results were expressed as mean ± standard error and analyzed using Excel 2010 and SPSS 22.0. The significance of differences among different data sets was analyzed using Duncan's multiple range test at a significance level of $p < 0.05$.

Abbreviations

LB: Late Bud;

FB: Floral Bud;

BR: Bract;

LE: Leaf;

WGCNA: Weighted correlation network analysis;

IAA: Indole-3-acetic acid ;

IPA: indole-3-pyruvic acid ;

SBP: Squamosa promoter binding protein;

PCA: Principal Component Analysis;

AP1: APETALA1;

FULL: FRUITFULL;

HEM11: glutamyl-tRNA reductase 1;

GSA: glutamate-1-semialdehyde 2,1-aminomutase;

HEM2: delta-aminolevulinic acid dehydratase;

DCUP: Uroporphyrinogen decarboxylase;

HEM4: uroporphyrinogen-III synthase;

HEM3: porphobilinogen deaminase;

HEM6: oxygen-dependent coproporphyrinogen-III oxidase;

POOC: protoporphyrinogen oxidase 1;

CHLH: Magnesium-chelatase subunit ;

CHLD: magnesium-chelatase subunit ;

CHLI: magnesium-chelatase subunitI;

CHLM: magnesium protoporphyrin IX methyltransferase;

CRD: dicarboxylate diiron protein;

PORA: protochlorophyllide oxidoreductase A;

DCVR: Divinyl chlorophyllide a 8-vinyl-reductase;

CHLG: chlorophyll synthase;

CHLP: geranylgeranyl reductase;

CAO: chlorophyllide a oxygenase;

SGR: STAY-GREEN protein ;

HCAR: coenzyme F420 hydrogenase family / dehydrogenase;

NYC1: NAD:P-binding Rossmann-fold superfamily protein;

PPH: pheophytinase;

CHLH: pheophorbide a oxygenase, chloroplastic;

RCCR: accelerated cell death ;

TRPX: anthranilate synthase alpha subunit 2;

ASB1: anthranilate synthase beta subunit 1;

PAT1: scarecrow-like protein 21 isoform X2 ;

PAI1: phosphoribosylanthranilate isomerase 1;

TRPC: Indole-3-glycerol phosphate synthase;

TRPA2: tryptophan synthase alpha chain isoform X1;

TRPB: hypothetical protein;

TAR1: tryptophan aminotransferase related 1;

TIR1: TRANSPORT INHIBITOR RESPONSE 1-like ;

YUC: Probable indole-3-pyruvate monooxygenase ;

AMI1: amidase 1; *ALDO2*:fructose-bisphosphate aldolase;

NCED2: nine-cis-epoxycarotenoid dioxygenase 2;

NCED1: 9-cis-epoxycarotenoid dioxygenase;

ABA2: NAD(P)-binding Rossmann-fold superfamily protein;

ALDO3: aldolase C.

Declarations

Ethics approval and consent to participate

Not applicable.

Consent for publication

Not applicable.

Availability of data and material

All data generated/analyzed during this study are included in this article and its supplementary files. The sequencing data associated with transcription profiles in this study have been deposited in the China National Center for Bioinformation database with accession number *GSA*:CRA006581(https://bigd.big.ac.cn/*GSA*/browse/CRA006581).

Competing interests

The authors declare that there are no competing interests

Funding

This study was conducted by Key project of Hunan Provincial Department of Education (22A0155); the Forest Bureau of Hunan Provence (XLKY2024); Hunan province education department project(22C1207, 22C1212).

Authors' contributions

X.D.L., Y.N.P., and Q.H.Z collected the sample and conceived and designed the study X.D.L., Y.W.M., Y.Q.H and J.L the Transcriptome analysis. X.D.L., J.L., M.L., X.Y.Y., Y.L.L., and F.X.C wrote the manuscript. All the authors reviewed and approved the manuscript.

Acknowledgments

Not applicable.

References

1. Alsamadany H. De novo leaf transcriptome assembly of *Bougainvillea spectabilis* for the identification of genes involves in the secondary metabolite pathways[J]. Gene, 2020, 746:144660.
2. Wu X, Gao R, Mao R, et al. Inducing bract-like leaves in *Arabidopsis* through ectopically expressing an *ASR* gene from the dove tree[J]. Industrial Crops and Products, 2022.
3. Anil S R, Devi A A, Asha K I, et al. Intraspecific inflorescence and palynological variations in the morphotypes of *Amorphophallus paeoniifolius*[J]. Genetic Resources and Crop Evolution, 2023(7):70.
4. Wang L, Ming L, Liao K, et al. Bract suppression regulated by the miR156/529-SPLs-NL1-PLA1 module is required for the transition from vegetative to reproductive branching in rice[J]. Molecular plant: S1674-2052(21)00158-1.
5. Xiao Y, Guo J, Dong Z, et al. Boundary domain genes were recruited to suppress bract growth and promote branching in maize[J]. Cold Spring Harbor Laboratory, 2021.

6. Neves B, Zanella C M, Kessous I M, et al. Drivers of bromeliad leaf and floral bract variation across a latitudinal gradient in the Atlantic Forest[J]. Journal of Biogeography, 2020, 47.
7. Koo S C, Bracko O, Park M S, et al. Control of lateral organ development and flowering time by the Arabidopsis thaliana MADS-box Gene AGAMOUS-LIKE6[J]. Plant Journal for Cell & Molecular Biology, 2010, 62(5):807-816.
8. Hou H, Tian M, Liu N, et al. Genome-wide analysis of MIKCC-type MADS-box genes and roles of CpFUL/SEP/AGL6 superclade in dormancy breaking and bud formation of *Chimonanthus praecox*[J]. Plant Physiology and Biochemistry, 2023.
9. Zhao Y H, Zhang X M, Li D Z . Development of the petaloid bracts of a paleoherb species, *Saururus chinensis*[J]. PLoS ONE, 2021, 16(9): e0255679.
10. Jiang Y, Wang M, Zhang R, et al. Identification of the target genes of AqAPETALA3-3 (AqAP3-3) in *Aquilegia coerulea* (Ranunculaceae) helps understand the molecular bases of the conserved and nonconserved features of petals[J]. The New phytologist, 2020, 227(4):1235-1248.
11. Schiessl K, Jose M Muiño, Sablowski R. *Arabidopsis* JAGGED links floral organ patterning to tissue growth by repressing Kip-related cell cycle inhibitors[J]. Proceedings of the National Academy of Sciences of the United States of America, 2014, 111(7):2830-2835.
12. Zhang W , Zhou Q , Lin J ,et al. Transcriptome analyses shed light on floral organ morphogenesis and bract color formation in *Bougainvillea*[J].BMC Plant Biology, 2022, 22(1):1-13.
13. Lan L, Zhao H Q, Xu S X, et al. A high-quality *Bougainvillea* genome provides new insights into the evolutionary history and pigment biosynthetic pathways in the Caryophyllales[J].Horticulture Research. 2023 ,10(8): uhad124.
14. B, Hammad Saleem A, et al. *Bougainvillea glabra* (choisy): A comprehensive review on botany, traditional uses, phytochemistry, pharmacology and toxicity[J]. Journal of Ethnopharmacology, 2020, 266.
15. Fonseca R, Carmen C, Lebrón R, et al. Insights into the functional role of tomato TM6 as a transcriptional regulator of flower development[J]. Horticulture Research, 2024(3):3.
16. Martínez-Fernández I, Fourquin C, Lindsay D, et al. Analysis of pea mutants reveals the conserved role of FRUITFULL controlling the end of flowering and its potential to boost yield[J]. Proceedings of the National Academy of Sciences, 2024, 121(15): e2321975121.
17. Liu X, Mao X, Chen J, Du Y, Jin W, Liu R, Zhou L, Qu Y. Transcriptomics Reveal an Integrated Gene Regulation Network of Early Flowering Development in an *Oil Sunflower* Mutant Induced by Heavy Ion Beam[J]. *Agriculture*, 2024, *14*, 449.
18. Fonseca R, Carmen C, Lebrón R, et al. Insights into the functional role of tomato TM6 as a transcriptional regulator of flower development[J]. Horticulture Research, 2024(3):3.
19. Landis J B, Barnett L L, Hileman L C. Evolution of petaloid sepals independent of shifts in B-class MADS box gene expression[J]. Development Genes & Evolution, 2012, 222(1):19-28.
20. Feng Y Y, Du H, Huang K Y, et al. Reciprocal expression of MADS-box genes and DNA methylation reconfiguration initiate bisexual cones in spruce[J]. Communications Biology, 2024, 7(1): 114.

21. Baranov D, Dolgov S, Timerbaev V. New Advances in the Study of Regulation of Tomato Flowering-Related Genes Using Biotechnological Approaches[J]. Plants, 2024, 13(3): 359.
22. Zhang J, Hu Z, Wang Y, et al. Suppression of a tomato SEPALLATA MADS-box gene, *SlCMB1*, generates altered inflorescence architecture and enlarged sepals[J]. Plant Science, 2018: S0168945217312207.
23. Zhang J , Hu Z , Yao Q ,et al. A tomato MADS-box protein, *SlCMB1*, regulates ethylene biosynthesis and carotenoid accumulation during fruit ripening[J]. Scientific Reports, 2018, 8(1). DOI:10.1038/s41598-018-21672-8.
24. Gao D, Zhang Q, Xu T, et al. Bioinformatics Identification and Expression Profiles of SBP Family Genes in Cucumber (*Cucumis sativus L.*)[J]. Plant Gene and Trait, 2024, 15.
25. Shaheen T, Rehman A, Abeed A H A, et al. Identification and expression analysis of SBP-Box-like (SPL) gene family disclose their contribution to abiotic stress and flower budding in pigeon pea (*Cajanus cajan*)[J]. Functional Plant Biology, 2024, 51(3).
26. Ma K, Zhao Y, Han L, et al. Genome-Wide Analysis of SPL Gene Family and Functional Identification of JrSPL02 Gene in the Early Flowering of Walnut[J]. Horticulturae, 2024, 10(2): 158.
27. Jiang X, Lubini G, Hernandes-Lopes J, et al. FRUITFULL-like genes regulate flowering time and inflorescence architecture in tomato[J]. The Plant Cell, 2022, 34(3): 1002-1019.
28. Wang X, Liu Z, Sun S, et al. SISTER OF TM3 activates FRUITFULL1 to regulate inflorescence branching in tomato[J]. Horticulture Research, 2021, 8.
29. Ye L X, Zhang J X, Hou X J, et al. A MADS-box gene CiMADS43 is involved in citrus flowering and leaf development through interaction with *CiAGL9*[J]. International Journal of Molecular Sciences, 2021, 22(10): 5205.
30. Zhang C H, Shangguan L F, Ma R J, et al. Genome-wide analysis of the *AP2/ERF* superfamily in peach (Prunus persica)[J]. Genet Mol Res, 2012, 11(4): 4789-4809.
31. Hwan L J, Joon K J, Ahn J H. Role of SEPALLATA3 (*SEP3*) as a downstream gene of miR156-SPL3-FT circuitry in ambient temperature-responsive flowering[J]. Plant signaling & behavior, 2012, 7(9): 1151-1154.
32. Cai J, Liu W, Li W, et al. Downregulation of miR156-targeted *PvSPL6* in switchgrass delays flowering and increases biomass yield[J]. Frontiers in Plant Science, 2022, 13: 834431.
33. Chen G, Li J, Liu Y, et al. Roles of the GA-mediated *SPL* gene family and miR156 in the floral development of Chinese chestnut (*Castanea mollissima*)[J]. International Journal of Molecular Sciences, 2019, 20(7): 1577.
34. Malhotra K, Kim S T, Batschauer A, et al. Putative blue-light photoreceptors from *Arabidopsis thaliana* and Sinapis alba with a high degree of sequence homology to DNA photolyase contain the two photolyase cofactors but lack DNA repair activity[J]. Biochemistry, 1995, 34(20):6892.
35. Keracka K, Sylwia, Mysliwa K, et al. Insight into the oligomeric structure of *PORA* from A. thaliana[J].Biochimica et biophysica acta: BBA: International journal of biochemistry, biophysics and molecular biololgy. Proteins and Proteomics, 2016, 1864(12):1757-1764.

36. Xing X, Ding Y, Jin J, et al. Physiological and Transcripts Analyses Reveal the Mechanism by Which Melatonin Alleviates Heat Stress in Chrysanthemum Seedlings[J]. Frontiers in Plant Science, 2021, 12:2012-.
37. Micha G, Anna S, Wojciech S, et al. Photoactive Protochlorophyllide-Enzyme Complexes Reconstituted with *PORA*, *PORB* and *PORC* Proteins of A. thaliana: Fluorescence and Catalytic Properties[J]. PLoS ONE, 2015, 10(2): e0116990-.
38. Uluisik S, Kıyak A, Kurt F, et al. STAY-GREEN (*SGR*) genes in tomato (*Solanum lycopersicum*): Genome-wide identification, and expression analyses reveal their involvements in ripening and salinity stress responses[J]. Horticulture, Environment, and Biotechnology, 2022, 63(4): 557-569.
39. Kasahara H. Current aspects of auxin biosynthesis in plants[J]. Bioscience Biotechnologyn & Biochemistry, 2016, 80(1): 34-42.
40. Chen Q, Dai X, De-Paoli H, et al. Auxin Overproduction in Shoots Cannot Rescue Auxin Deficiencies in *Arabidopsis* Roots[J]. Plant & Cell Physiology, 2014, 55(6):1072-9.
41. Mashiguchi K, Tanaka K, Sakai T, et al. The main auxin biosynthesis pathway in *Arabidopsis*[J]. Proceedings of the National Academy of Sciences, 2011.
42. Anna, N, Stepanova, et al. The *Arabidopsis YUCCA1* Flavin Monooxygenase Functions in the Indole-3-Pyruvic Acid Branch of Auxin Biosynthesis[J]. The Plant Cell, 2011, 23(11):3961-3973.
43. Zhang M, Liu Y, Chen Z, et al. Progress in Fruit Cracking Control of Gibberellic Acid and Abscisic Acid[J]. Forests, 2024, 15(3): 547.
44. Shkryl Y N, Vasyutkina E A, Gorpenchenko T V, et al. Salicylic acid and jasmonic acid biosynthetic pathways are simultaneously activated in transgenic Arabidopsis expressing the rolB/C gene from Ipomoea batatas[J]. Plant Physiology and Biochemistry, 2024: 108521.
45. Yanru H, Xiao H, Milian Y, et al. The Transcription Factor INDUCER OF CBF EXPRESSION1 Interacts with ABSCISIC ACID INSENSITIVE5 and DELLA Proteins to Fine-Tune Abscisic Acid Signaling during Seed Germination in Arabidopsis[J]. The Plant Cell, (7):7,2024-04-11.

Figures

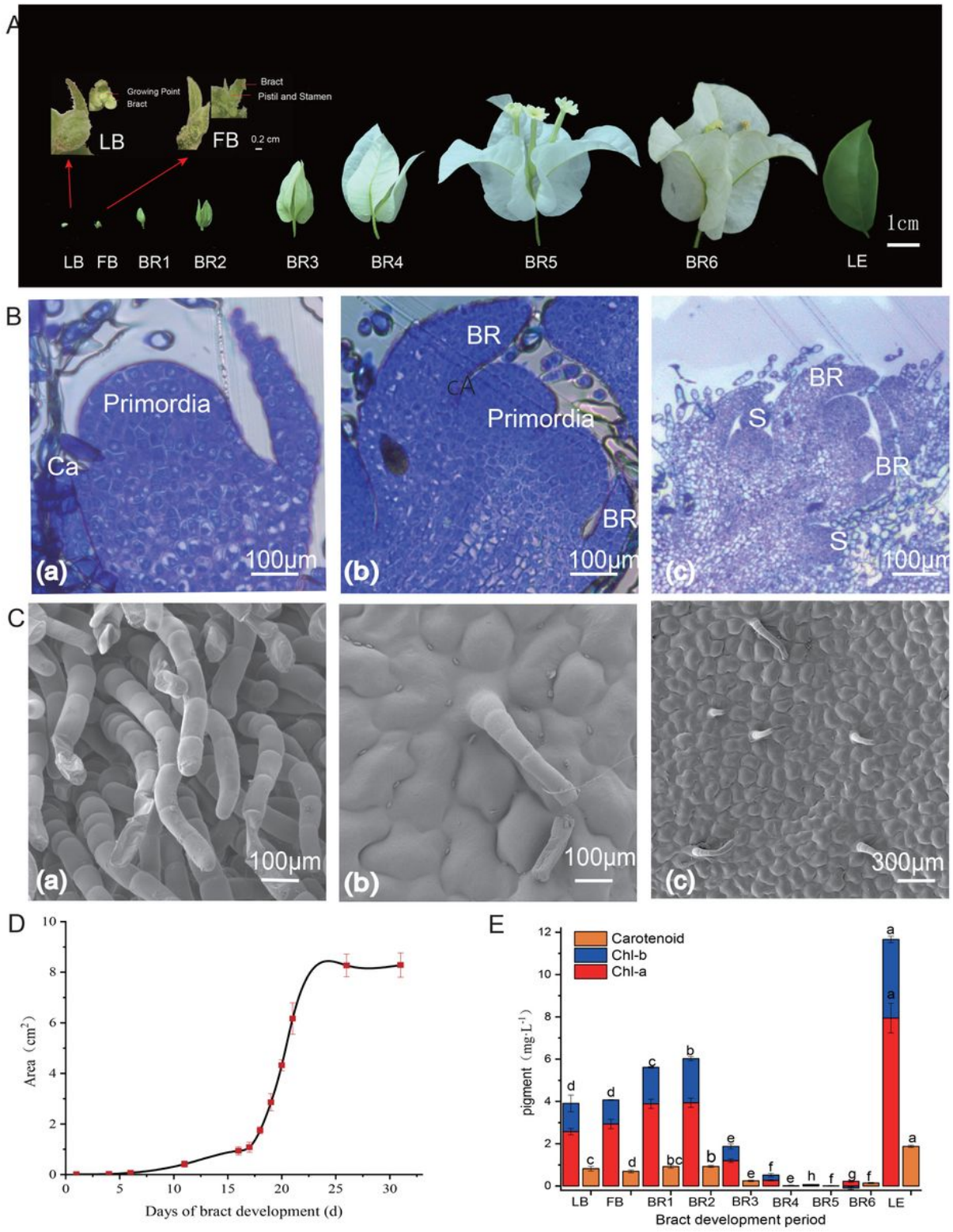

Figure 1

Morphostructural and chlorophyll changes during bract development in *B. glabra.* **A** *B. glabra* leaf buds, bracts 7 developmental periods, and leaf sampling periods; **B** Resin section of *B. glabra* during bud development. (a) Inflorescence primordium differentiation stage. (b) Late stage of floral primordial differentiation. (c)The organs of the third chakra begin to develop consecutively; **C** Electron microscope scan of the bract development process of *B. glabra.* (a) Electron microscope scan of bracts from the BR1

period. (b) Bract fluff shedding. (c) Electron microscope scan of bracts at the time of BR5. **D** Changes in bract area during bract development in *B. glabra*. **E** Chlorophyll and carotene content of leaf buds, bracts and leaves at seven developmental stages of *B.glabra*.

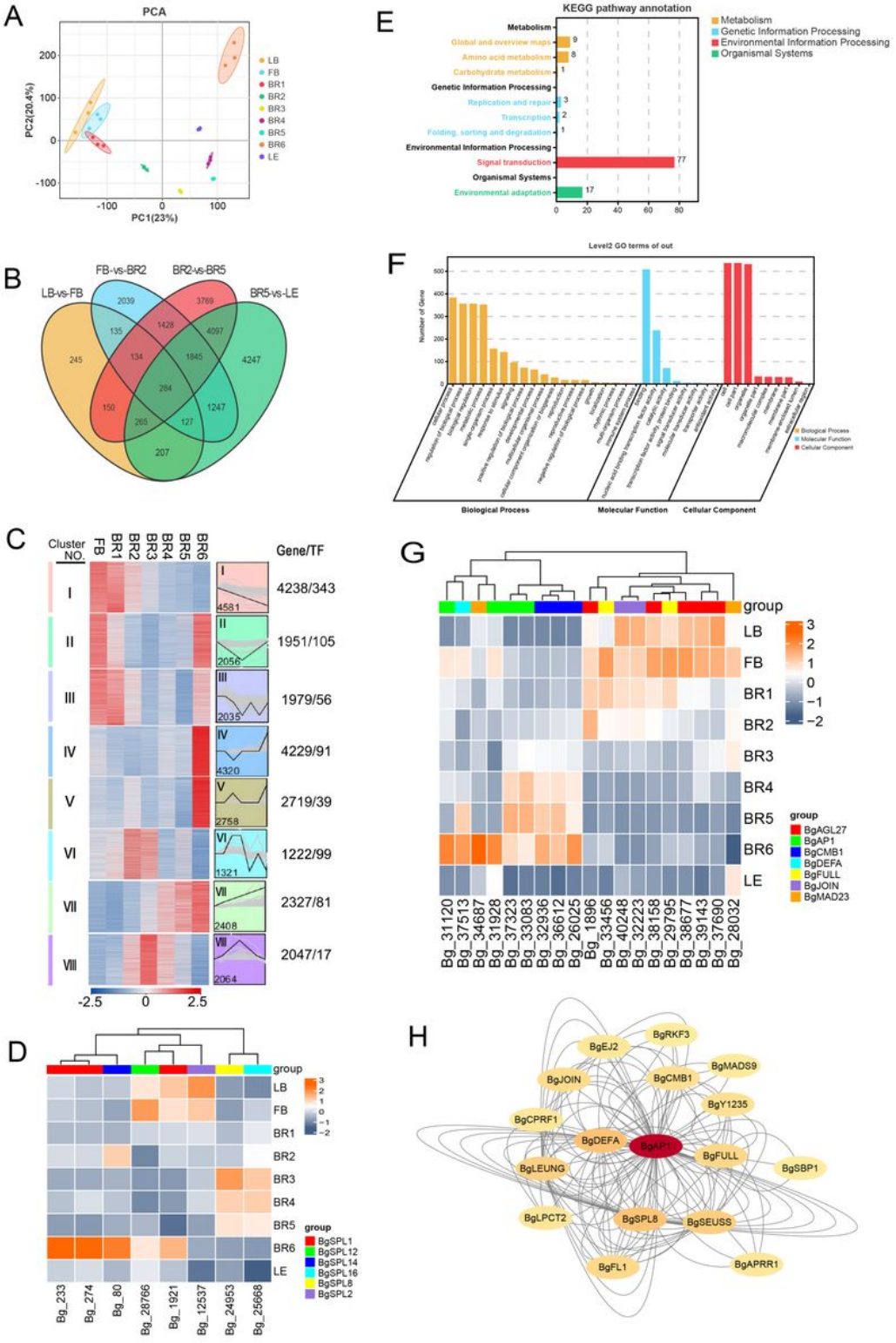

Figure 2

Analysis of genetic differences. **A** Sample FPKM values PCA analysis plot. **B** Differential gene Wayne plots for LB/FB, FB/BR2, BR2/BR5, BR5/LE.**C** STEM trend analysis plot. **D** Differential transcription factor KEGG enrichment analysis plot. **E** Differential transcription factor GO enrichment analysis plot. **F** Heatmap of SPLS family members of differential genes in significant expression trends. **G**Heat map of differential gene MADS-box family members in significant expression trend. **H** Differential protein network interactions graph.

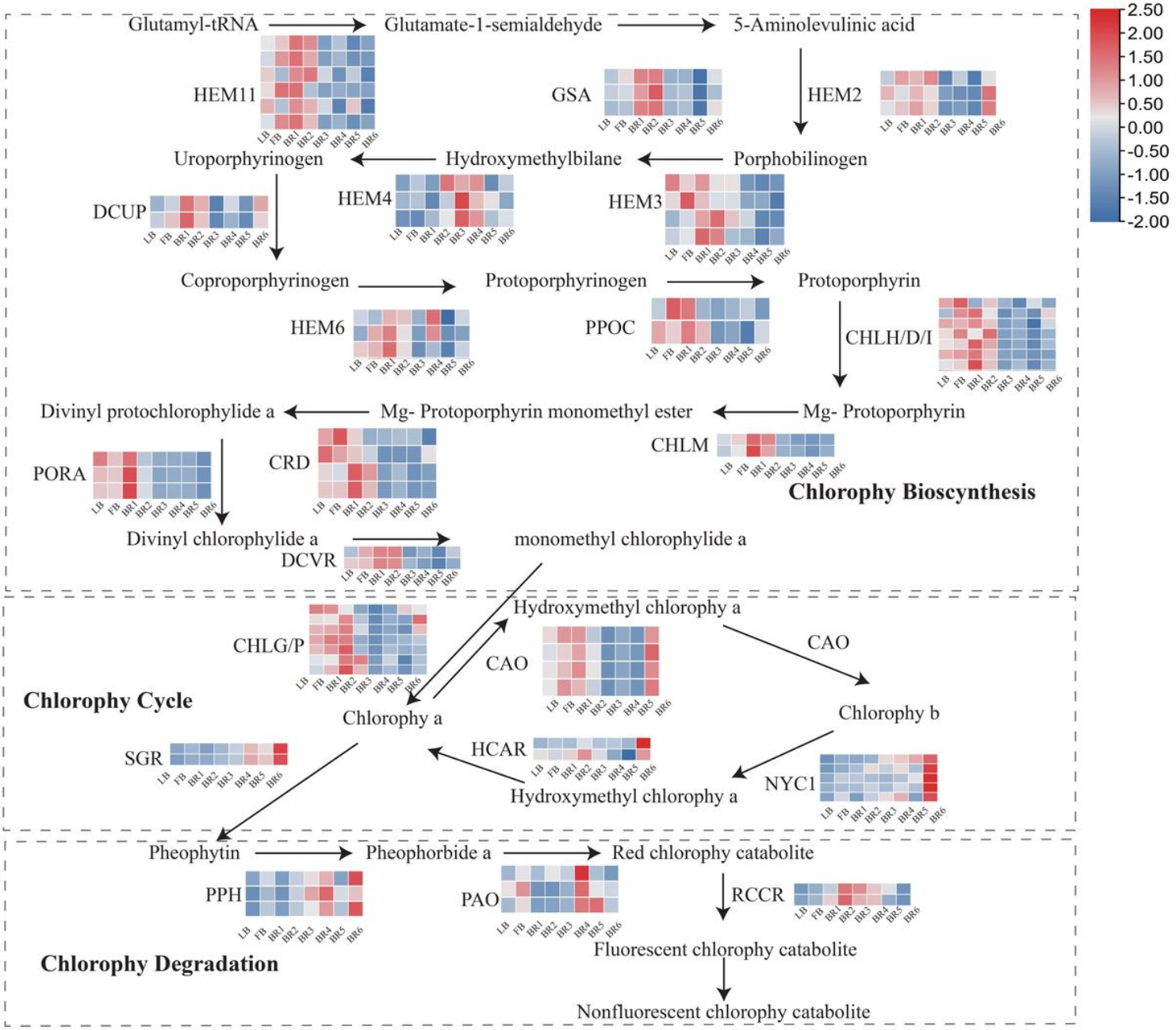

Figure 3

Chlorophyll metabolism pathway.*HEM11*(glutamyl-tRNA reductase 1);*GSA*(glutamate-1-semialdehyde 2,1-aminomutase); HEM2(delta-aminolevulinic acid dehydratase); *DCUP*(Uroporphyrinogen decarboxylase); *HEM4*(uroporphyrinogen-III synthase); *HEM3*(porphobilinogen deaminase); *HEM6*(oxygen-dependent

coproporphyrinogen-III oxidase); *ppoc*(protoporphyrinogen oxidase 1); *CHLH*(Magnesium-chelatase subunit *CHLH*); *CHLD*(magnesium-chelatase subunit *CHLD*); *CHLI*(magnesium-chelatase subunitI); *CHLM*(magnesium protoporphyrin IX methyltransferase); *CRD*(dicarboxylate diiron protein); *PORA*(protochlorophyllide oxidoreductase A); *DCVR*(Divinyl chlorophyllide a 8-vinyl-reductase); *CHLG*(chlorophyll synthase); *CHLP*(geranylgeranyl reductase); *CAO*(chlorophyllide a oxygenase); *SGR*(protein STAY-GREEN 1); *HCAR*(coenzyme F420 hydrogenase family / dehydrogenase); *NYC1*(NAD(P)-binding Rossmann-fold superfamily protein); PPH(pheophytinase); *PAO*(pheophorbide a oxygenase, chloroplastic); RCCR(accelerated cell death)

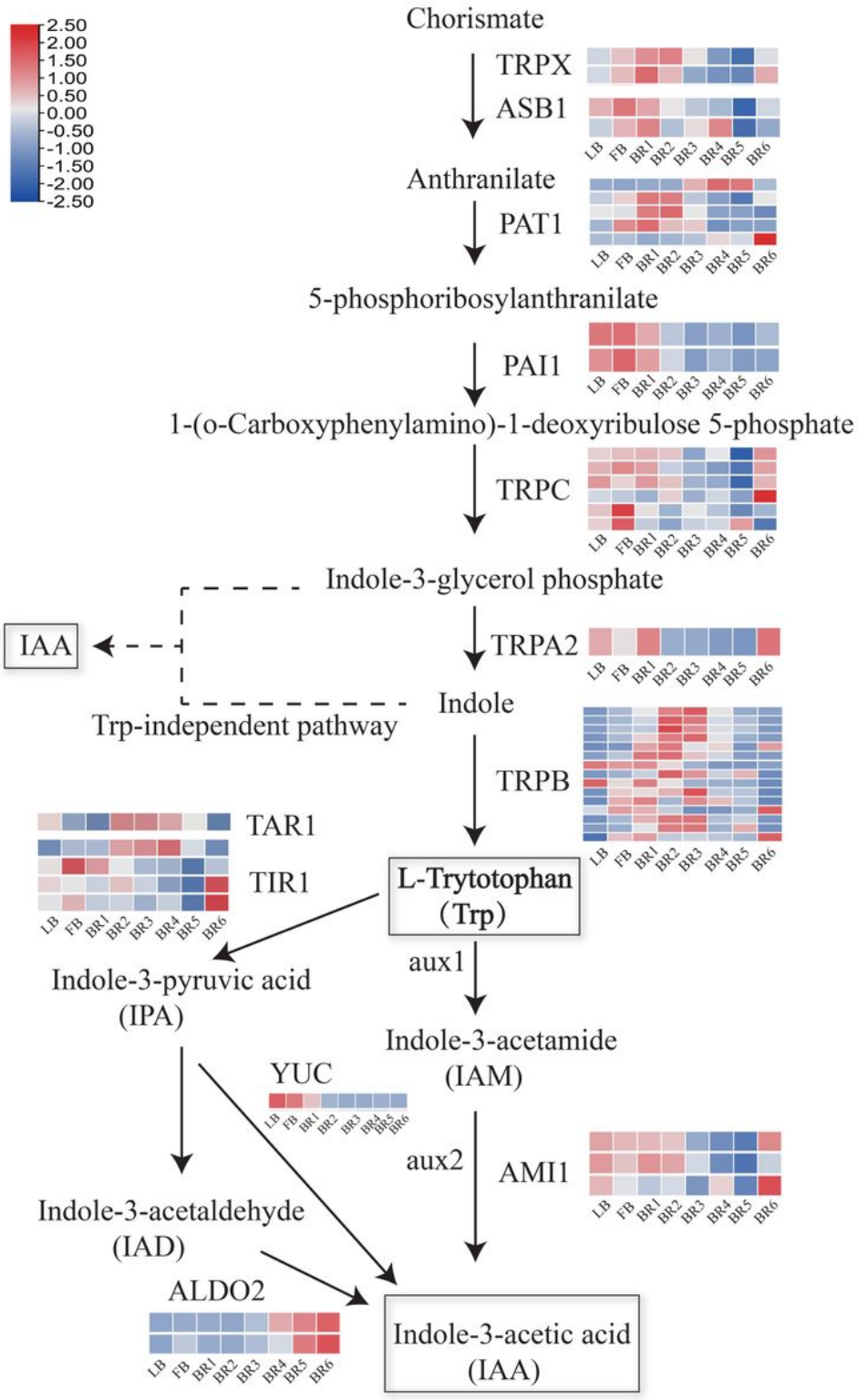

Figure 4

Expression analysis of plant growth hormone synthesis genes in *B. glabra* bract development stages. *TRPX*(anthranilate synthase alpha subunit 2); *ASB1*(anthranilate synthase beta subunit 1); *PAT1*(scarecrow-like protein 21 isoform X2) *PAI1*(phosphoribosylanthranilate isomerase 1);TRPC(Indole-3-glycerol phosphate synthase); *TRPA2*(tryptophan synthase alpha chain isoform X1); *TRPB*(hypothetical protein) ; *TAR1*(tryptophan aminotransferase related 1); *TIR1*(TRANSPORT INHIBITOR RESPONSE 1-like);

YUC(Probable indole-3-pyruvate monooxygenase); *AMI1*(amidase 1);*ALDO2*(fructose-bisphosphate aldolase)

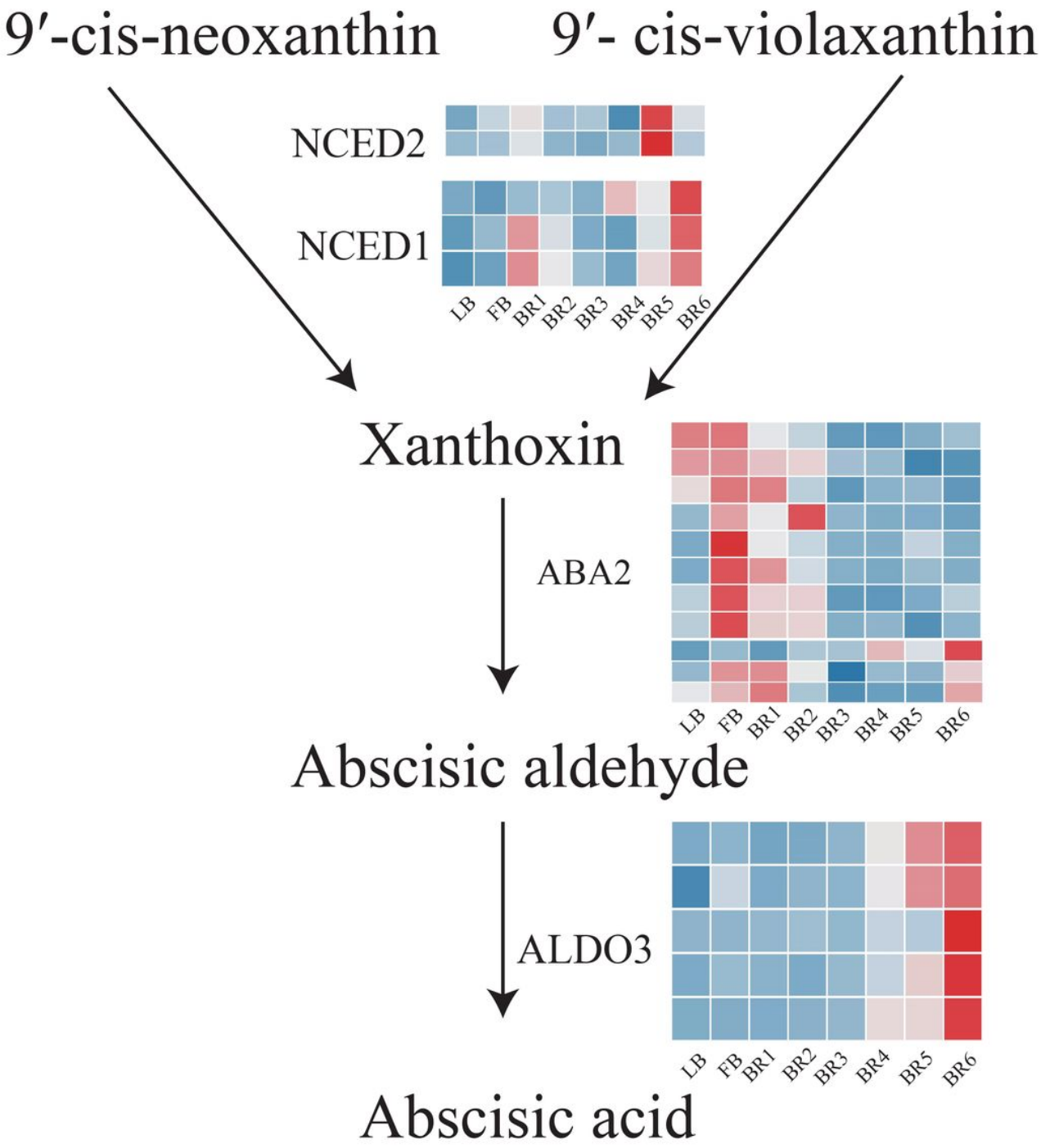

Figure 5

Expression analysis of plant abscisic acid synthesis genes at *B. glabra* bract developmental stages. *NCED2* (nine-cis-epoxycarotenoid dioxygenase 2); *NCED1*(9-cis-epoxycarotenoid dioxygenase); *ABA2*(NAD(P)-binding Rossmann-fold superfamily protein); *ALDO3*(aldolase C).

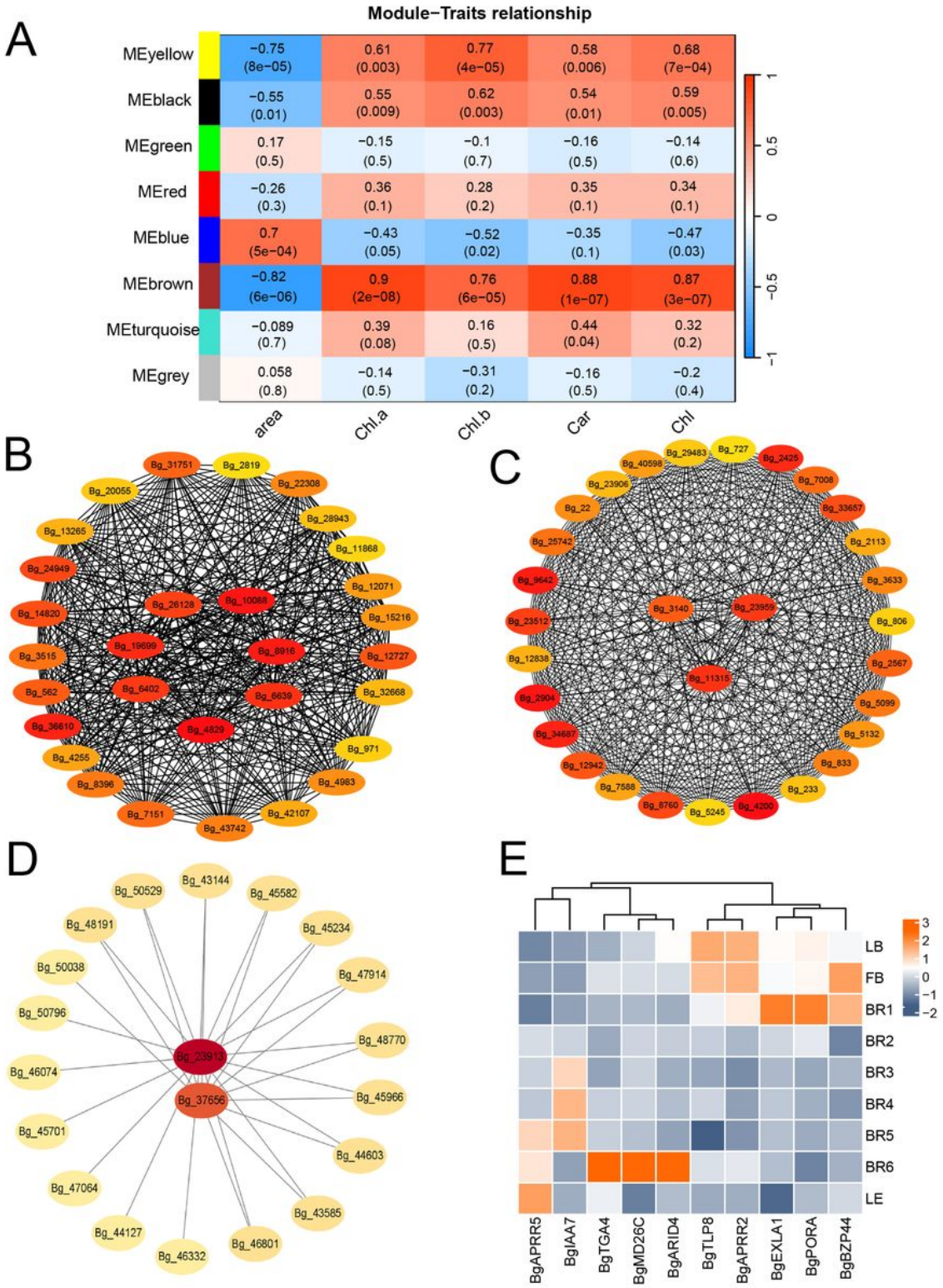

Figure 6

Weighted correlation network analysis of transcripts. **A** WGCNA analysis with module-physiological growth indicator associations. Each row corresponds to a module. The names of the modules are shown on the left. Each column corresponds to a specific physiological growth indicator. The colour of each cell at the row-column intersection indicates the correlation coefficient between the module and the sample. High correlations between specific modules and samples are indicated in red. **B** Interaction diagram of

the gene network of the co-expressed gene ME blue module transcription factor HUB. **C** ME brown module transcription factor HUB gene network interaction plot. **D** ME brown module structural gene HUB gene network inter-operation diagram. **E** Heatmap of related HUB gene expression.

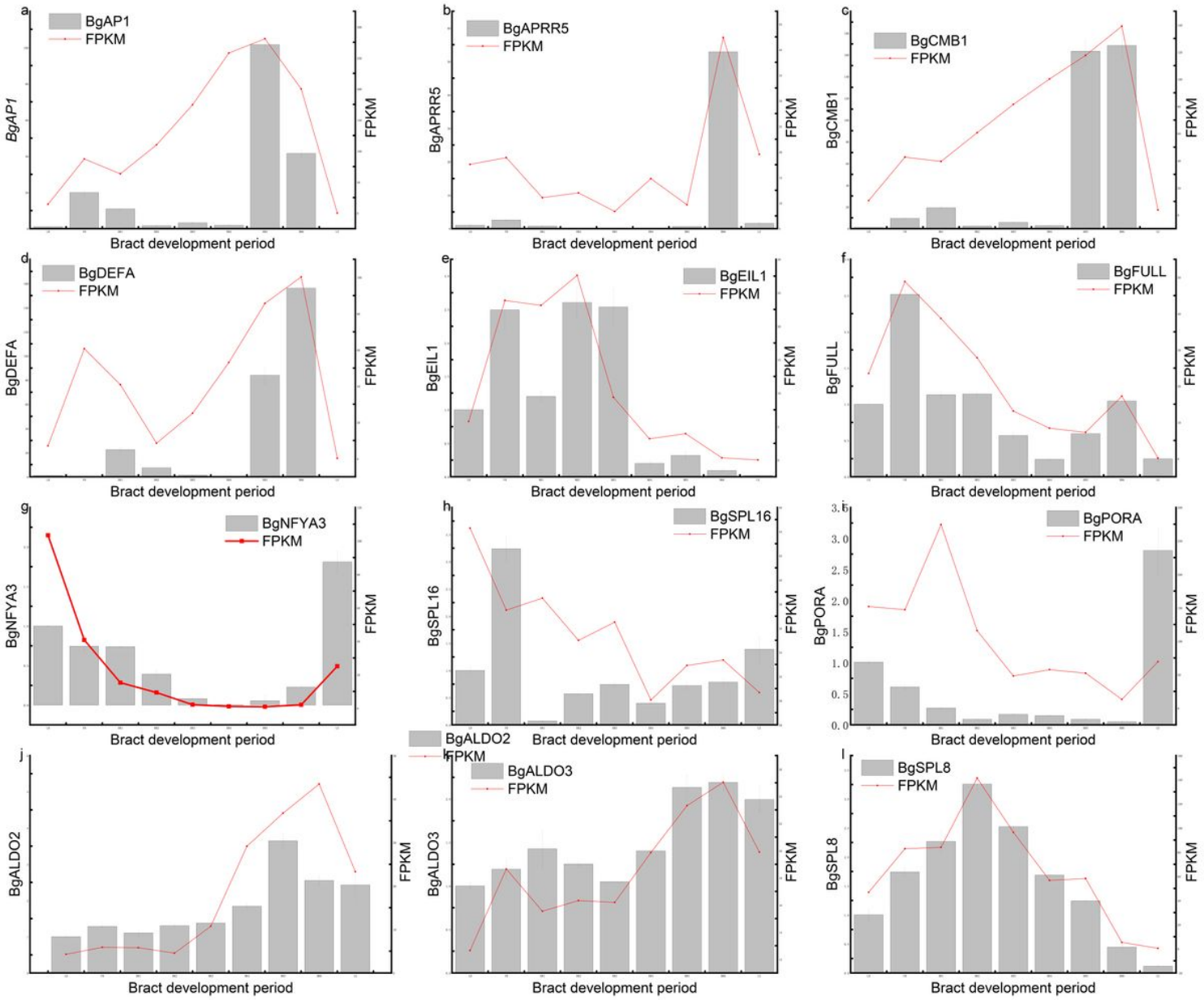

Figure 7

Candidate gene qRT-PCR identification FPKM values were derived from *B. glabra* transcriptome data. actin gene was used as an internal control. Ib as a control was assigned an arbitrary value of 1.0. The data represent three biological replicates and their mean values, and the error line represents the standard deviation of the three biological replicates.

Supplementary Files

This is a list of supplementary files associated with this preprint. Click to download.

- attachment.docx